

Published in final edited form as:

J Fluoresc. 2003 November ; 13(6): 453–457. doi:10.1023/B:JOFL.0000008055.22336.0b.

Fluorescence Spectral Properties of Indocyanine Green on a Roughened Platinum Electrode: Metal-Enhanced Fluorescence

Chris D. Geddes¹, Alexandr Parfenov², David Roll², Md. Jamal Uddin², and Joseph R. Lakowicz^{2,3}

¹Institute of Fluorescence and Center for Fluorescence Spectroscopy, Medical Biotechnology Center, University of Maryland Biotechnology Institute, Baltimore, Maryland. ²Department of Biochemistry and Molecular Biology, Center for Fluorescence Spectroscopy, University of Maryland School of Medicine, 725 West Lombard Street, Baltimore, Maryland 21201.

Abstract

The interactions of fluorophores with noble metal particles can modify their emission spectral properties, a relatively new phenomenon in fluorescence. We subsequently examined indocyanine green (ICG), which is widely used in medical testing and imaging, in close proximity to an electrically roughened platinum electrode. The emission intensity and lifetimes were decreased about 2-fold on the roughened surface as compared to a smooth Pt surface, and the photostability about the same. Platinum does not appear promising for metal enhanced fluorescence, at least for long wavelength fluorophores.

Keywords

Roughened platinum electrode; metal-enhanced fluorescence; radiative decay engineering; indocyanine green

INTRODUCTION

In recent publications we described the effects of metallic silver particles and colloids on nearby fluorophores [1–5]. Excited state fluorophores behave as oscillating dipoles, which interact with free electrons in metals [6–8]. These interactions can increase the radiative decay rate, Γ of fluorophores resulting in many desirable effects such as, increased quantum yields, Q_m , and decreased lifetimes, τ_m Fig. 1. These effects are likely to result in many applications of metal-enhanced fluorescence, such as in medical diagnostics and imaging [1]. To date our studies are limited to silver particles and colloids [1–5], plus one study of gold colloids [9]. Gold is attractive for metal-enhanced fluorescence (MEF) because it is chemically more stable than silver. However, the visible absorption of gold is known to quench fluorescence [10].

In an effort to identify other metals for MEF we examined metallic platinum. The surface of a strip of platinum (in essence an electrode) was roughened by oscillating voltages, Fig. 2, analogous to the procedure used for surface enhanced Raman scattering (SERS) [11,12]. We found minimal effects of platinum on the long wavelength fluorophore indocyanine green

(ICG), which is widely used in medical testing and diagnostics. These results suggest platinum will not be useful for metal-enhanced fluorescence, at least for long wavelength fluorophores.

Experimental Materials

Indocyanine Green (ICG) and human serum albumin (HSA) were obtained from Sigma and used without further purification. The platinum foil (electrode) was roughened as described below. Concentrations of ICG and HSA were determined using extinction coefficients of $\epsilon(780)=130,000\text{ cm}^{-1}$ and $\epsilon(278)\text{ nm}=37,000\text{ cm}^{-1}$, respectively. Glass microscope slides were cleaned by immersion in 30% v/v H_2O_2 and 70% v/v H_2SO_4 for 48 hr and then washed in distilled water. The glass slides were used to cover the platinum electrode in a sandwich type conformation so as to keep the sample moist. Binding the ICG-HSA to the electrode was accomplished by soaking in a 30 μM ICG, 60 μM HSA solution overnight, followed by rinsing with water to remove the unbound material. Both the roughened and unroughened platinum surfaces were coated with the labelled HSA, which is known to passively adsorb to noble metal surfaces and form an $\approx 4\text{ nm}$ thick monolayer [5], allowing us to study the fluorescence spectral properties of noncovalent ICG-HSA complexes in the absence and presence of roughened platinum. In addition, we have previously shown that HSA coatings are ideal “bio-spacers” for MEF [5], rendering a population of ICG molecules out of the close proximity metal-quenching range, Fig. 1, and into the range which affords for an increase in fluorophore radiative decay rate [1–5].

EXPERIMENTAL METHODS

Excitation and observation of the sandwiched samples were made by the front face configuration (Fig. 3). Steady state emission spectra were recorded using a SLM 8000 spectrofluorometer with excitation using a Spectra Physics Tsunami Ti: Sapphire laser in the CW (nonpulsed) mode with an attenuated as required $\approx 200\text{ mW}$ 760 nm output. This enabled the samples to be photo-bleached as required, i.e. for matching the initial steady state intensities or using the same excitation power.

Platinum foil, 0.1 mm thick, 99.99% was obtained from Aldrich. A standard 10 mm cuvette was filled with 1.0M H_2SO_4 and 2 platinum foil electrodes were installed. The platinum electrodes were roughened by an electrical oxidation and reduction process, which involved potentiodynamically cycling the voltage between the electrodes for 20 ms in the range +1.2 V to -0.4 V, for 1 min, Fig. 2. The current was generated using a Lab 200, ID instruments, Australia, current generator. The electrode was then washed with doubly distilled deionised water for ca. 3 min and then the whole electrode was coated with ICG-HSA, as described above. For the roughening procedure, only half the Pt electrode was immersed in 1.0 M H_2SO_4 , allowing the unroughened portion to act as a control sample when coated with ICG-HSA. It should be noted that a detailed literature is also available for the preparation of roughened metal electrodes [13,14].

Time-resolved intensity decays were measured using reverse start-stop time-correlated single-photon counting. Vertically polarized excitation at $\approx 760\text{ nm}$ was obtained using a mode-locked argon-ion pumped, cavity dumped Pyridine 2 dye laser with a 3.77 MHz repetition rate. The instrumental response function, determined using the experimental geometry in Fig. 3, was typically $<50\text{ ps}$ fwhm. The emission was collected at the magic angle (54.7°), using a long pass filter (Edmund Scientific), which cut off wavelengths below 780 nm, with an additional $830\text{ nm} \pm 10\text{ nm}$ interference filter. Carefully undertaken control experiments with both roughened platinum, and protein only coated roughened platinum, showed that scattered light was alleviated from the measurements.

DATA ANALYSIS

The intensity decays were analyzed in terms of the multi-exponential model:

$$I(t) = \sum_i \alpha_i \exp(-t/\tau_i) \quad (1)$$

where α_i are the amplitudes and τ_i the decay times, $\sum \alpha_i = 1.0$. The fractional contribution of each component to the steady-state intensity is given by:

$$f_i = \frac{\alpha_i \tau_i}{\sum_j \alpha_j \tau_j} \quad (2)$$

The mean lifetime of the excited state is given by:

$$\bar{\tau} = \sum_i f_i \tau_i \quad (3)$$

and the amplitude-weighted lifetime is given by:

$$\langle \tau \rangle = \sum_i \alpha_i \tau_i \quad (4)$$

The values of α_i and τ_i were determined by non-linear least squares impulse reconvolution with a goodness-of-fit χ_r^2 criterion.

RESULTS

Figure 4 shows the emission spectra of ICG-HAS on a smooth and roughened platinum surface. We found no significant effect, about 2-fold lower intensity on the roughened surface as compared to the smooth surface. Since it is likely that the roughened surface binds more ICG-HSA than the smooth surface, the extent of quenching is probably even higher.

We examined the time-dependent intensity decays of ICG-HSA on the two platinum surfaces, Fig. 5 and Table 1. The lifetime of ICG on the roughened platinum electrode was shorter, as expected, as compared to the unroughened electrode, i.e. 36 and 55 ps respectively. It is known that decreased lifetimes can result in increased photostability [15]. Presumably this occurs because a shortened lifetime allows less time in the excited state per excitation de-excitation cycles. We examined the intensity of ICG-HSA on the two platinum surfaces with continuous illumination, Fig. 6. When observed with the same illumination intensity, ICG-HSA photobleaches more rapidly on the smooth as compared to the roughened surface. Alternatively we adjusted the incident intensities to obtain the same initial emission intensity from both surfaces, which required approximately 2-fold lower intensity incident on the unroughened sample. In this case (Fig. 6, bottom) ICG-HAS still appeared to be more photostable. From the areas under these curves we estimate that roughly the same total emission can be obtained from ICG-HSA on the smooth and roughened surfaces.

CONCLUSIONS

Platinum surfaces display high chemical stability and thus promising for metal enhanced fluorescence. For the long wavelength probe ICG we did not observe useful spectral changes on platinum. However, the plasmon absorption of platinum occurs at shorter wavelengths, typically <300 nm [16,17], and platinum may thus find use with shorter wavelength fluorophores, or even weakly fluorescing bio-molecules. Further Investigations are underway.

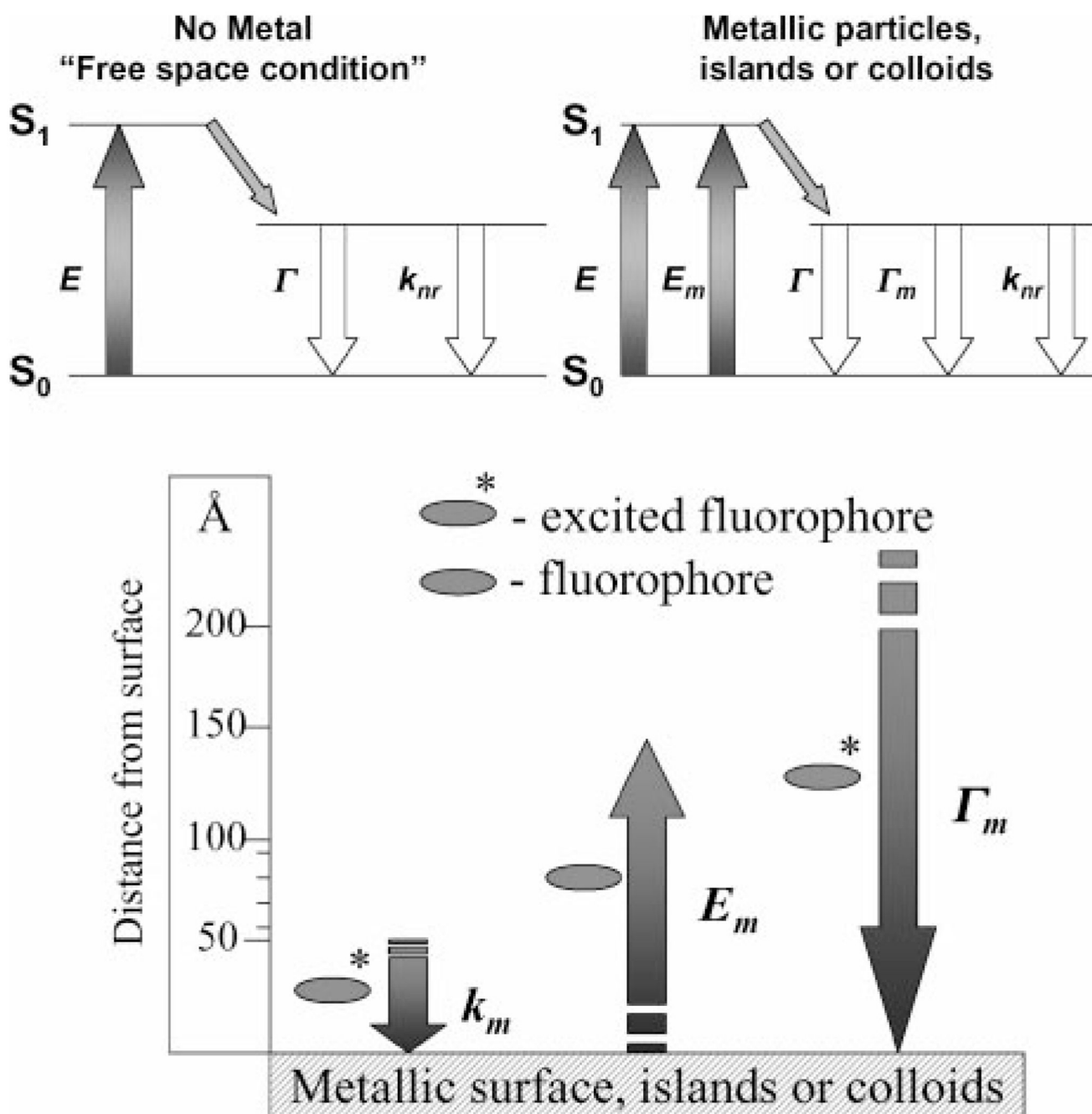
Acknowledgments

This work was supported by the National Center for Research Resources, RR-08119, and the National Institute of Biomedical Imaging and Bioengineering, EB-00682.

REFERENCES

1. Lakowicz JR. Radiative decay engineering: Biophysical and biomedical applications. *Anal. Biochem* 2001;298:1–24. [PubMed: 11673890]
2. Lakowicz JR, Shen Y, D'Auria S, Malicka J, Fang J, Gryczynski Z, Gryczynski I. Radiative decay engineering 2. Effects of silver island films on fluorescence intensity, lifetimes, and resonance energy transfer. *Anal. Biochem* 2002;301:261–277. [PubMed: 11814297]
3. Lakowicz JR, Shen YB, Gryczynski Z, D'Auria S, Gryczynski I. Intrinsic fluorescence from DNA can be enhanced by metallic particles. *Biochem. Biophys. Res. Commun* 2001;286:875–879. [PubMed: 11527380]
4. Malicka J, Gryczynski I, Kusba J, Shen YB, Lakowicz JR. Effects of metallic silver particles on resonance energy transfer in labeled bovine serum albumin. *Biochem. Biophys. Res. Commun* 2002;294:886–892. [PubMed: 12061790]
5. Geddes CD, Cao H, Gryczynski I, Gryczynski Z, Fang J, Lakowicz JR. Metal-enhanced fluorescence (MEF) due to silver colloids on a planar surface: Potential applications of indocyanine green to *in vivo* imaging. *J. Phys. Chem. A* 2003;107(18):3443–3449.
6. Chance RR, Prock A, Silbey R. Molecular fluorescence and energy transfer near interfaces. *Adv. Chem. Phys* 1978;37:1–65.
7. Gersten JI, Nitzan A. Accelerated energy transfer between molecules near a solid particle. *Chem. Phys. Lett* 1984;104:31–37.
8. Gersten J, Nitzan A. Spectroscopic properties of molecules interacting with small dielectric particles. *J. Chem. Phys* 1981;75:1139–1152.
9. Geddes CD, Cao H, Lakowicz JR. Enhanced photostability of ICG in close proximity to gold colloids. *Spectrochim. Acta: A* 2003;59(11):2611–2617.
10. Dubertret B, Calame M, Libchaber AJ. Single-mismatch detection using gold-quenched fluorescent oligonucleotides. *Nat. Biotechnol* 2001;19:365–370. [PubMed: 11283596]
11. Fleischmann M, Hendra PJ, McQuillan AJ. Raman spectra of pyridine adsorbed at a silver electrode. *Chem. Phys. Letts* 1974;26(2):163–166.
12. Roth E, Hope GA, Schweinsberg DP, Kiefer W, Fredericks PM. Simple technique for measuring surface-enhanced fourier transform Raman spectra of organic compounds. *Appl. Spectrosc* 1993;47(11):1794–1800.
13. Huanq QB, Cai WW, Mao BM, Liu F, Tian Z. Surface Raman spectra of pyridine and hydrogen on bare platinum electrodes. *J. Electroanal. Chem* 1996;415(1/2):175–178.
14. Cao P, Bin G, Tian Z. Surface enhanced raman scattering of pyridine on platinum and nickel electrodes in nonaqueous solutions. *Chem. Phys. Lett* 2002;366:440–446.
15. Jovin, TM.; Arndt-Jovin, DJ. *Cell Structure and Function by Microscopyfluorometry*. Kohen, E.; Hirschberg, JG.; Ploem, JS., editors. London: Academic Press; 1989. p. 99-117.
16. Yguerabide J, Yguerabide EE. Light-scattering submicroscopic particles as highly fluorescent analogs and their use as tracer labels in clinical and biological applications—1. Theory. *Anal. Biochem* 1998;262:137–156. [PubMed: 9750128]

17. Yguerabide J, Yguerabide EE. Light-scattering submicroscopic particles as highly fluorescent analogs and their use as tracer labels in clinical and biological applications—2. Experimental characterization. *Anal. Biochem* 1998;262:157–176. [PubMed: 9750129]

**Figure 1.**

Top—Classical Jablonski diagram for the *free space condition* and the modified form in the presence of metallic particles, islands or colloids. E —excitation, E_m —metal enhanced excitation rate and Γ_m —radiative rate in the presence of metal. Bottom—Predicted distance dependencies for a metallic surface on the transitions of a fluorophore. The metallic surface can cause Förster like quenching with a rate, k_m , can concentrate the incident field, E_m , and can increase the radiative decay rate, Γ_m .

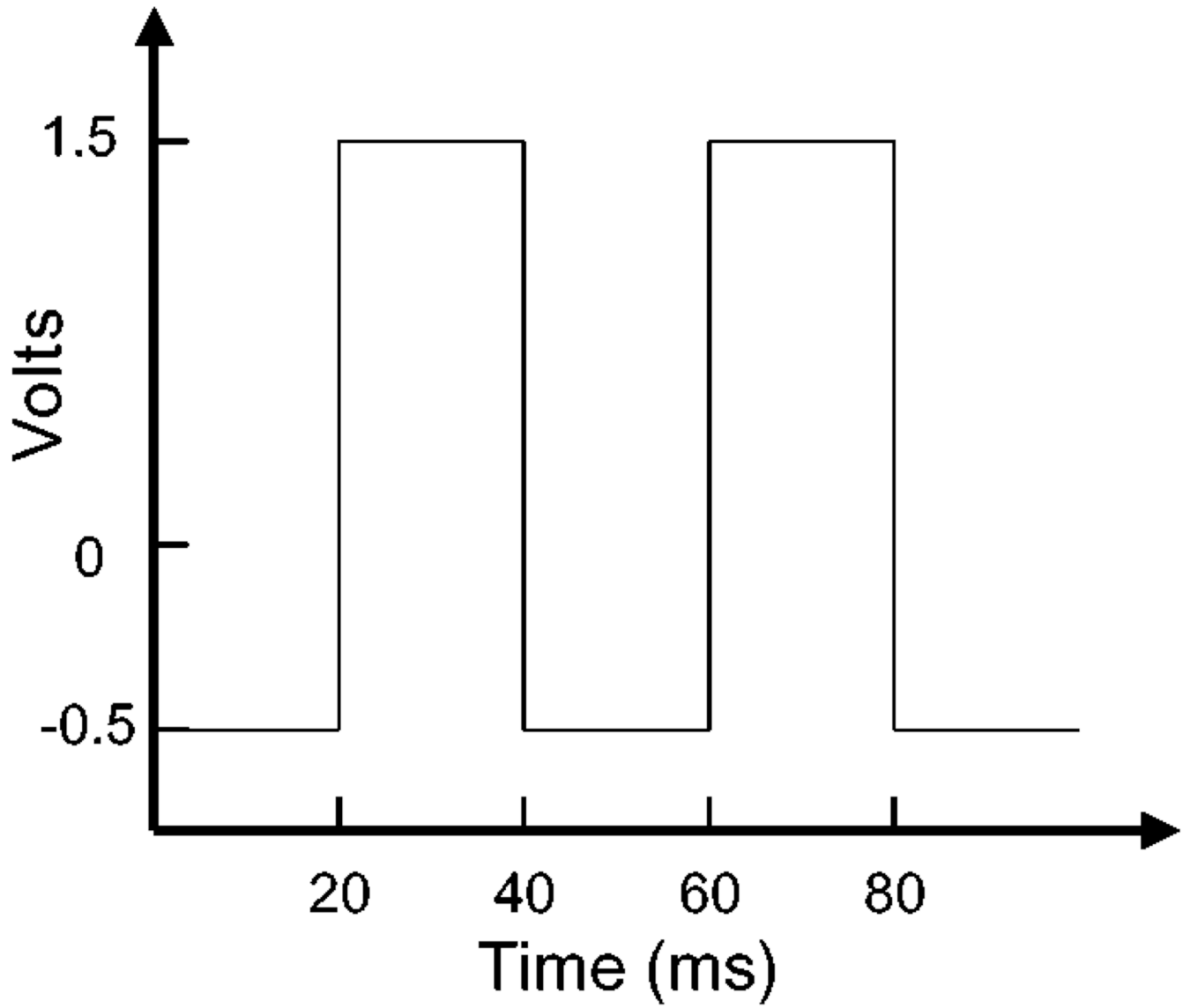
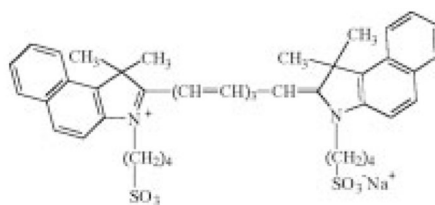


Figure 2.
Periodic voltage used to roughen the platinum electrode.



ICG Molecular Structure

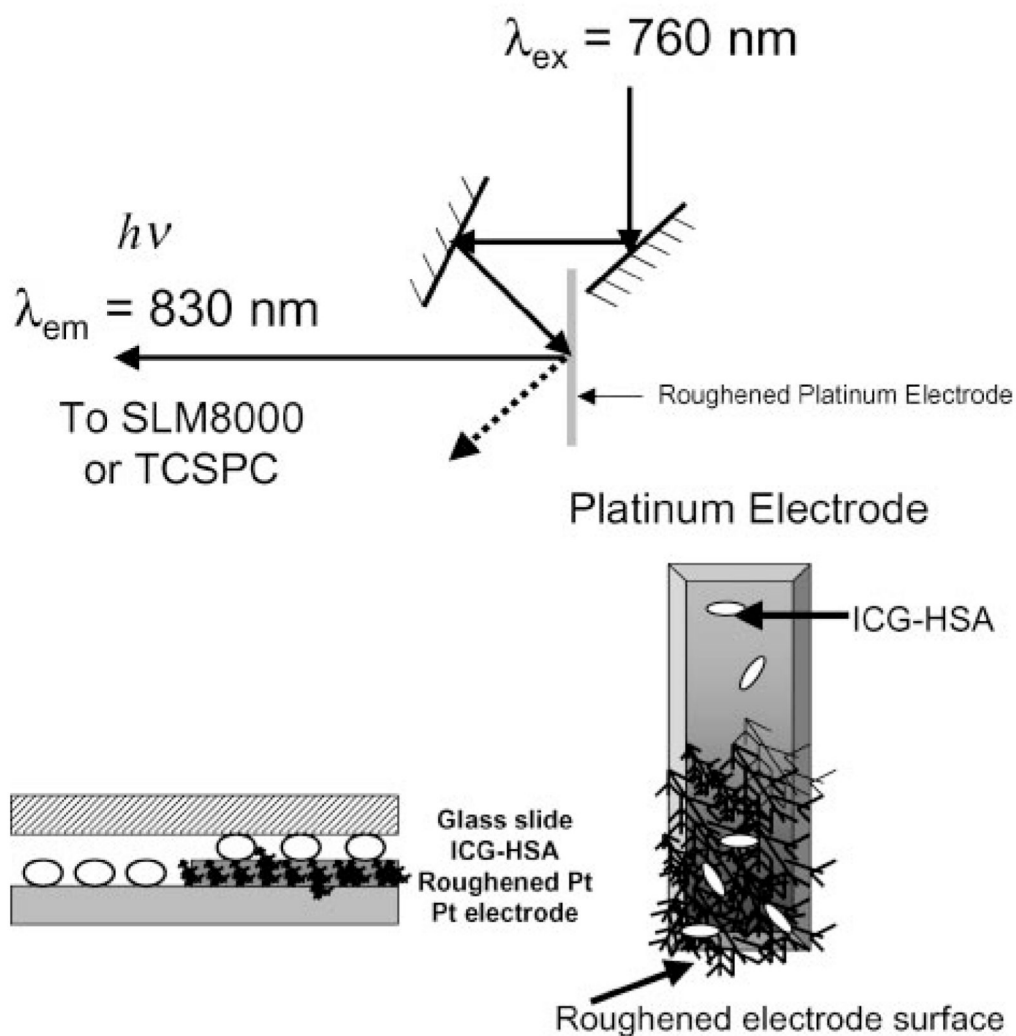


Figure 3. Experimental geometry. The glass slide (cover slip) on the Pt electrode was used to keep the protein layer moist.

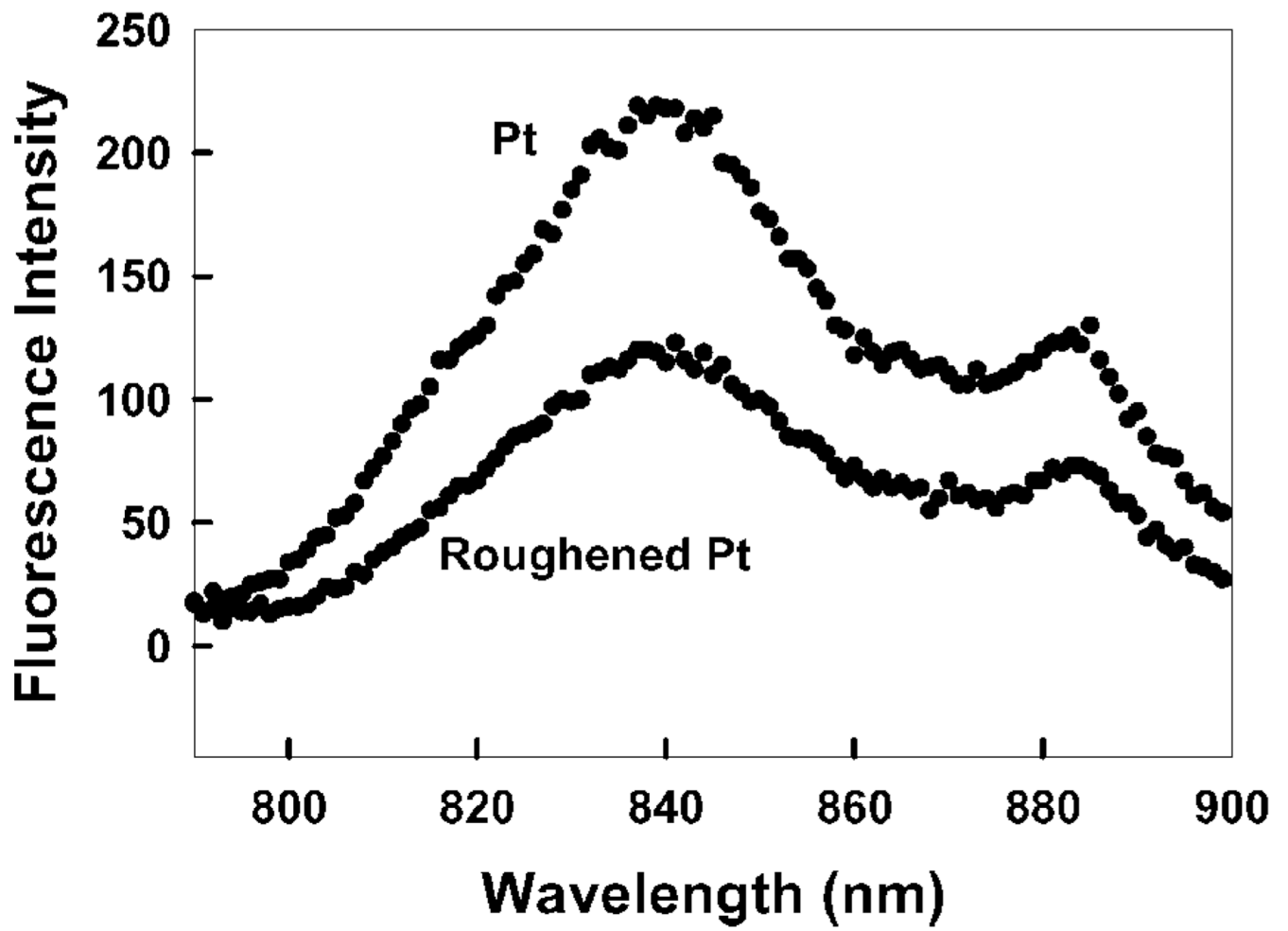


Figure 4.
ICG emission on both roughened and unroughened platinum.

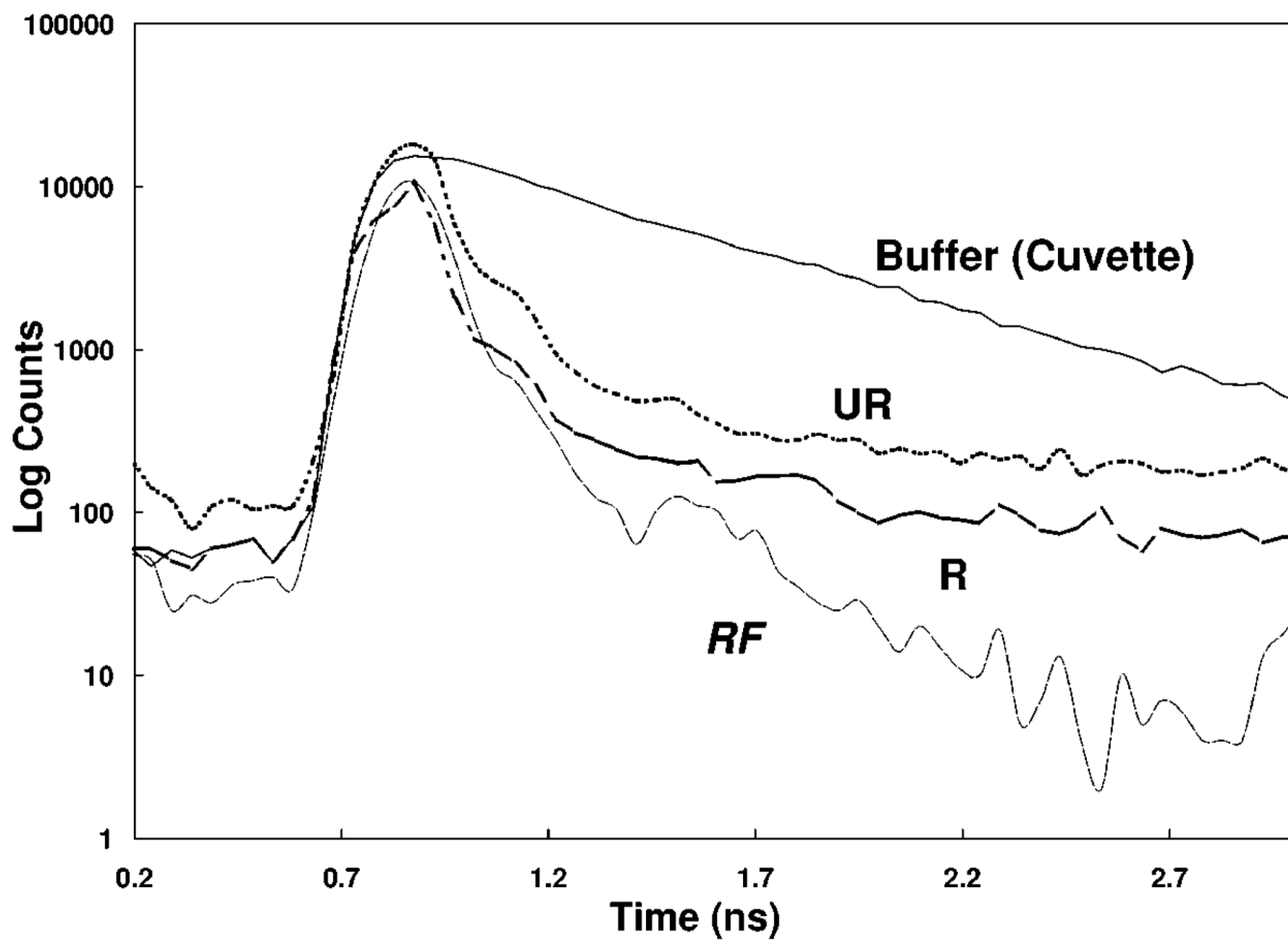


Figure 5. Complex intensity decays of ICG-HSA on unroughened and roughened platinum. RF—Instrumental response function.

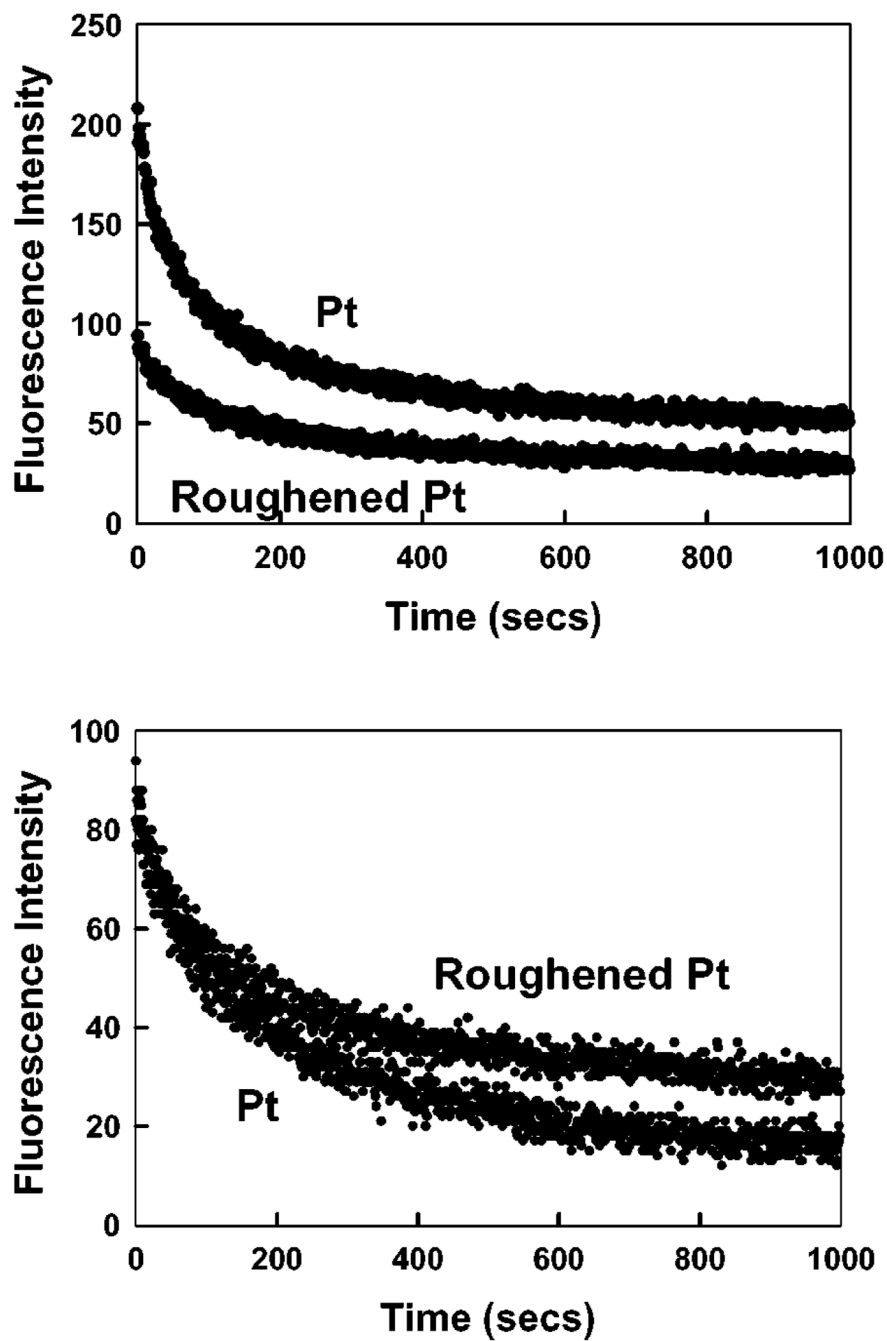


Figure 6. Photostability of ICG-HSA on roughened and unroughened platinum (Pt), measured using the same excitation power at 760 nm (Top) and with power *adjusted* to give the same initial fluorescence intensities (Bottom). In all measurements vertically polarized excitation was used. The fluorescence emission was observed at the magic angle, i.e. 54.70.

Table I

Analysis of the Intensity Decay of ICG-HSA Measured Using the Reverse Start-Stop Time-Correlated Single Photon Counting Technique and the Multi-Exponential Model

Sample	a_i	τ_i (ns)	f_i	$\bar{\tau}$ (ns)	$\langle \tau \rangle$ (ns)	χ_R^2
In buffer	0.158	0.190	0.05	—	—	1.40
	0.842	0.615	0.95	0.592	0.548	
Roughened Pt	1.0	0.036	1.0	0.036	0.036	2.54
Unroughened Pt	1.0	0.055	1.0	0.055	0.055	1.47

Note. Using the multiexponential model offered no notable improvement in the χ^2 for fitting.